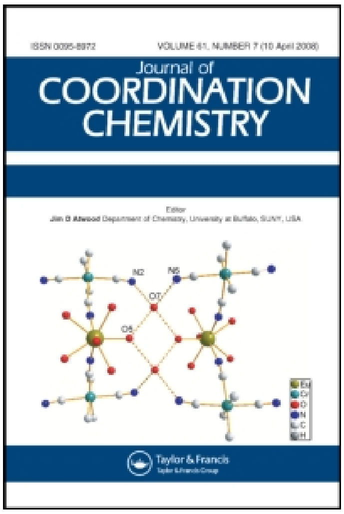

Journal of Coordination Chemistry
Publication details, including instructions for authors and subscription information:
http://www.informaworld.com/smpp/title~content=t713455674

Transition metal complexes of acetamidomalondihydroxamate: synthesis, spectral, thermal and electrochemical studies

Fatih Yilmaz[a]; Veysel T. Yilmaz[a]; Saim Topcu[a]
[a] Ondokuz Mayis University, Faculty of Arts and Sciences, Department of Chemistry, 55139 Kurupelit, Samsun, Turkey

To cite this Article Yilmaz, Fatih , Yilmaz, Veysel T. and Topcu, Saim(2004) 'Transition metal complexes of acetamidomalondihydroxamate: synthesis, spectral, thermal and electrochemical studies', Journal of Coordination Chemistry, 57: 6, 525 — 534

To link to this Article: DOI: 10.1080/00958970410001696843

URL: http://dx.doi.org/10.1080/00958970410001696843

J. Coord. Chem., Vol. 57, No. 6, 15 April 2004, pp. 525–534

Taylor & Francis
Taylor & Francis Group

TRANSITION METAL COMPLEXES OF ACETAMIDOMALONDIHYDROXAMATE: SYNTHESIS, SPECTRAL, THERMAL AND ELECTROCHEMICAL STUDIES

FATIH YILMAZ, VEYSEL T. YILMAZ* and SAIM TOPCU

Ondokuz Mayis University, Faculty of Arts and Sciences, Department of Chemistry
55139 Kurupelit, Samsun, Turkey

(Received 16 May 2003; Revised 4 September 2003; In final form 4 March 2003)

Acetamidomalondihydroxamate (K_2AcAMDH) and its manganese(II), iron(II), cobalt(II), nickel(II), copper(II) and zinc(II) complexes were synthesized and characterized by elemental analysis, UV–VIS, IR and magnetic susceptibility. The pK_{a1} and pK_{a2} values of the dihydroxamic acid in aqueous solution were found to be 8.0 ± 0.1 and 9.7 ± 0.1. The dihydroxamate anion AcAMDH behaves as a tetradentate bridging ligand through both hydroxamate groups, forming complexes with a metal to ligand ratio of 1 : 1 in the solid state. The FTIR spectra and thermal decompositions of the ligand and its metal complexes were recorded. The redox behavior of the complexes was investigated in aqueous solution by square wave voltammetry and cyclic voltammetry at neutral pH. In contrast to the solid state, in solution the copper(II) and zinc(II) ions form stable complex species with a metal to ligand ratio of 1 : 2. The iron(II) and nickel(II) complexes show a two-electron irreversible reduction behavior, while the copper(II) and zinc(II) complexes undergo reversible electrode reactions. The stability constants of the complexes were determined by square wave voltammetry.

Keywords: Acetamidomalondihydroxamate; Metal complexes; Square wave voltammetry; Cyclic voltammetry

INTRODUCTION

Hydroxamic acids function as both weak acids and weak bases. Hydroxamate-type siderophores generally possess two or three hydroxamate functional groups. Biochemical interest in hydroxamate siderophores and their analogues exists because of their role in iron-transport phenomena [1,2]. Hydroxamic acids also have important functions as inhibitors of enzymatic activity, which was proved to be due to hydroxamate coordination to the metal centres of the enzymes [3,4]. The coordination chemistry of hydroxamic acids and their derivatives was reviewed by Chatterjee [5]

---

*Corresponding author. E-mail: vtyilmaz@omu.edu.tr

ISSN 0095-8972 print: ISSN 1029-0389 online
DOI: 10.1080/00958970410001696843

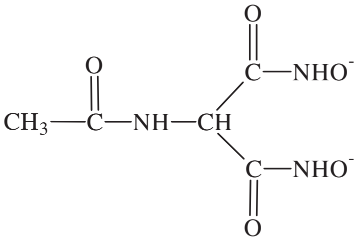

FIGURE 1 Molecular structure of AcAMDH.

and Kurzak *et al.* [6], and it was concluded that hydroxamic acids usually behave as bidentate (O,O′) chelates through the carbonyl and deprotonated hydroxyl oxygen atoms [7].

We have been involved in the synthesis and the spectral and thermal characterization of new monohydroxamic acids and their metal complexes [8–11]. The present article reports the synthesis and full characterization of the potassium salt of acetamidomalondihydroxamate (K_2AcAMDH) (Fig. 1) as well as its coordination behavior towards some of the first-row bivalent transition metal ions, iron(II), cobalt(II), nickel(II), copper(II) and zinc(II), in solution and in the solid state using spectral, thermal and electrochemical techniques.

EXPERIMENTAL

Materials and Methods

Starting materials were purchased from commercial suppliers and used without further purification. Electronic spectra were measured on a Unicam UV2 spectrophotometer in *N*-methylformamide (NMF) solutions of the complexes in the range 200–900 nm. IR spectra were recorded on a Mattson FTIR spectrophotometer as KBr pellets in the frequency range 4000–300 cm^{-1}. Magnetic susceptibility measurements were carried out using a Sherwood Scientific MXI model Gouy magnetic balance at room temperature. The C, H, N and S contents were measured on a Vario EL Elemental Analyzer. Thermal analysis curves (TG, DTA and DTG) were obtained using a Rigaku TG8110 thermal analyzer in a flowing nitrogen atmosphere. A sample size of *ca* 10 mg and a heating rate of 10°C min^{-1} were used.

The fully protonated form of AcAMDH was obtained by acidifying an aqueous solution of K_2AcAMDH, and dissociation constants (pK_a) of AcAMDH were determined by alkalimetric titration of three samples (1×10^{-3} M) at 25 ± 0.1°C using a Jenway 3040 model ion analyzer.

Electrochemical Measurements

Electrochemical measurements were performed using a Metrohm 757 VA Computrace model voltammetric analyzer. The cell with a three-electrode setup was used: a hanging mercury drop electrode (working electrode), a platinum wire auxiliary electrode and an Ag/AgCl reference electrode. Square wave voltammetry (SWV) voltammograms were taken with voltage step of 0.004 V, amplitude 50 mV, scan rate 200 mV s^{-1} and frequency 50 Hz, while cyclic voltammetry (CV) voltammograms were recorded from 0.15 to −1.40 V using different scan rates. In DCP polarograms, the potential step and drop time were chosen as 0.004 V and 1 s, respectively. A 0.10 M KNO_3 solution was used as supporting electrolyte. All solutions were purged with pure and water-saturated nitrogen for 5 min prior to each voltammetric run.

Electrochemical measurements were performed at different buffer solution and pH values, and these preliminary experiments showed that a pH value of about 7 and a KNO_3 supporting electrolyte are necessary for obtaining clear voltammograms and well-defined cathodic peak potential values (E_{pc}) for most of the metal complexes investigated. The manganese(II), iron(II), cobalt(II), nickel(II), copper(II) and zinc(II) complexes of AcAMDH were generated *in situ* by stepwise addition of 100 μL ligand (1×10^{-3} M) to a 5.40×10^{-5} M solution of the metal in a 0.10 M KNO_3 solution.

Synthesis of the Potassium Salt of AcAMDH

$NH_2OH \cdot HCl$ (5.29 g, 75 mmol) dissolved in 30 mL methanol was neutralized with an equimolar amount of KOH dissolved in 30 mL methanol and the solution was filtered to remove solid KCl. Acetamidomalonic acid diethyl ester (5.43 g, 25 mmol) dissolved in methanol was mixed with the NH_2OH solution and stirred for 15 min. A solution of KOH (3.12 g, 50 mmol) dissolved in 30 mL methanol was added dropwise to the resulting reaction mixture and the solution was stirred overnight. The potassium salt of acetamidomalondihydroxamate (K_2AcAMDH) was filtered, washed with methanol and acetone, and finally air-dried at room temperature. Scheme 1 outlines the synthesis of the dihydroxamate ligand.

Preparation of the Solid Metal Complexes

The complexes were prepared by addition of a 10 mL aqueous solution of K_2AcAMDH (0.57 g, 2 mmol) to 10 mL aqueous solutions of metal salts [$MnSO_4 \cdot H_2O$, $FeSO_4 \cdot 7H_2O$, $CoSO_4 \cdot 7H_2O$, $NiCl_2 \cdot 6H_2O$, $CuSO_4 \cdot 5H_2O$, $Zn(CH_3COO)_2 \cdot 2H_2O$] (2 mmol). After a short time of stirring, the solutions yielded the respective solid metal complexes, which were filtered, washed with water several times and dried in air. Only the nickel(II) complex did not precipitate during complexation and KCl in the solution was precipitated by adding methanol, as the nickel(II) complex is soluble in methanol. The methanolic solution was separated and the nickel(II) complex was precipitated by adding diethyl ether to the solution.

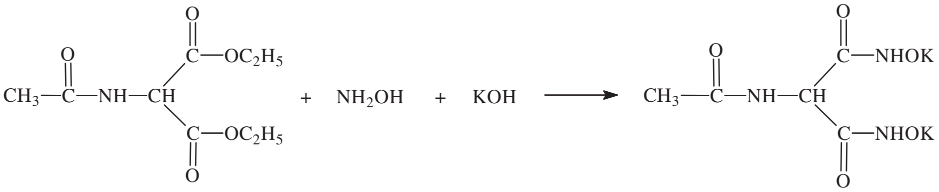

SCHEME 1 Synthesis of the potassium salt of the dihydroxamate ligand, K_2AcAMDH.

RESULTS AND DISCUSSION

Synthesis and Properties

The new dihydroxamate ligand was prepared as its potassium salt (potassium acetamidomalondihydroxamate, K_2AcAMDH) by the direct reaction of acetamidomalonic acid diethyl ester with hydroxylamine and potassium hydroxide as shown in Scheme 1. As well as the AcAMDH ligand, its solid metal complexes were obtained in good yields (over 70%) and the elemental analyses conformed to the proposed formulas given in Table I. K_2AcAMDH was found to be somewhat hygroscopic when exposed to air and the formula of the salt left in air is estimated as $K_2AcAMDH \cdot 1.5H_2O$. The molar ratio of M : ligand in the solid complexes was found to be 1 : 1. The complexes contain variable amounts of lattice water as estimated by TG and DTA (Table III). The solid metal complexes are stable in air and decompose at the temperatures given in Table I. They do not dissolve in water but are significantly soluble in NMF and slightly soluble in DMSO.

Of course, the structure of the solid metal complexes could be determined by single-crystal X-ray diffractometry, but as they do not dissolve in common solvents many attempts to prepare single crystals of the complexes failed.

Dissociation Constants

AcAMDHA in the acid form is diprotic due to the presence of two hydroxamic acid protons, and the dissociation constants were estimated from titration data within the pH range 3–11. Two readily detectable proton dissociations were observed and the pK_{a1} and pK_{a2} values were found to be 8.0 ± 0.1 and 9.7 ± 0.1, respectively. The dihydroxamic acid dissociation constants are comparable with those reported for the other dihydroxamic acids [12,13,15]. pK_{a1} would be expected to be lower than pK_{a2} and the difference between the two pK_a values ($pK_{a2} - pK_{a1}$) should be around 0.6 for a diprotic acid with two equivalent acid sites [14]. The large difference (1.7) found between the two pK_a values is due to a strong intramolecular hydrogen bond

TABLE I Analytical data for $K_2AcAMDH \cdot 1.5H_2O$ and the metal complexes

Compound	*Colour*	*FW*	*Decomp. temp. (°C)*	*Anal. Found (Calcd.) (%)*			*Yield (%)*
				C	*H*	*N*	
$K_2AcAMDH \cdot 1.5H_2O$	White	293.3	140	20.1	2.9	13.7	91
$K_2C_5H_{10}N_3O_{6.5}$				(20.5)	(3.4)	(14.3)	
$MnAcAMDH \cdot 5.5H_2O$	White	343.2	170	17.5	5.4	11.9	68
$MnC_5H_{17}N_3O_{10.5}$				(17.5)	(5.3)	(12.2)	
$FeAcAMDH \cdot 3H_2O$	Red–brown	299.0	125	20.1	4.4	14.0	88
$FeC_5H_{13}N_3O_8$				(19.8)	(4.0)	(13.8)	
$CoAcAMDH \cdot 2H_2O$	Brown	284.1	140	21.4	3.9	14.6	78
$CoC_5H_{11}N_3O_7$				(21.1)	(3.9)	(14.8)	
$NiAcAMDH \cdot H_2O$	Green	265.8	120	22.2	3.5	15.3	71
$NiC_5H_9N_3O_6$				(22.6)	(3.4)	(15.8)	
$CuAcAMDH \cdot H_2O$	Dark green	270.7	184	21.8	3.1	15.1	83
$CuC_5H_9N_3O_6$				(22.2)	(3.3)	(15.5)	
$ZnAcAMDH \cdot 2.5H_2O$	White	299.5	172	19.7	4.1	13.4	85
$ZnC_5H_{12}N_3O_{7.5}$				(20.0)	(4.0)	(13.6)	

between the two hydroxamic acid units within the same molecule and this interaction decreases pK_{a1} and increases pK_{a2} [13].

Spectral and Magnetic Characterization

Table II summarizes selected IR data of the free ligand and the solid metal complexes. The absorption band centred at 3284 cm^{-1} is due to the NH group of the free dihydroxamate ligand. As well as the ν(NH) bands, the hydrogen-bonded ν(OH) absorption bands of lattice or ligand water molecules occur as a broad band in the spectra of the metal complexes. In the spectrum of the ligand, the strong absorption bands at 1647 and 1560 cm^{-1} characterize the amide and hydroxamate carbonyl groups, respectively. The IR spectra of all the metal complexes resemble each other and IR spectra of K_2AcAMDH $\cdot$ 1.5H_2O and MnAcAMDH $\cdot$ 5.5H_2O are shown in Fig. 2. In the metal complexes, the carbonyl absorption bands of the dihydroxamate ligand shift significantly to lower frequency by about 20–40 cm^{-1} with respect to the free ligand, indicating coordination of the hydroxamate carbonyl oxygen in addition to the negatively charged oxygen of the same group.

Electronic spectral data are listed in Table II. K_2AcAMDH $\cdot$ 1.5H_2O shows an intense and complex band with mainly three maxima centred at 229, 248 and 274 nm due to $n \rightarrow \pi^*$ and $\pi \rightarrow \pi^*$ transitions in the UV region. The absorption bands of the intraligand transitions in the metal complexes are observed in condensed form with one to three λ_{max}. The broad bands with low intensity in the range 400–800 nm are assigned to d–d transitions, suggesting that all the metal complexes are high-spin. The room temperature magnetic moments are in good agreement with tetrahedral or octahedral coordination as given in Table II.

Thermal Analysis

Thermoanalytical data including decomposition ranges, DTA$_{max}$ and mass loss values of the potassium salt of the ligand and solid metal complexes are summarized

TABLE II Spectral[a] and magnetic data for K_2AcAMDH $\cdot$ 1.5H_2O and the metal complexes

Compound	*ν(NH)*	*ν(CH)*	*ν(CO) (amide)*	*ν(CO) (hydroxamate)*	*ν(CN)*	*λ_{max} (nm)*				*μ_{eff}[b] (BM)*
						L			*d–d*	
K_2AcAMDH $\cdot$ 1.5H_2O	3284 m	3053 w	1647 s	1560 s	1377 m	229	248	274	–	–
MnAcAMDH $\cdot$ 5.5H_2O	3250 m	3034 w	1642 s	1518 s	1369 m	235	249	273	–	5.43 (5.92)
FeAcAMDH $\cdot$ 3H_2O	3261 sh	3020 sh	1653 s	1539 s	1373 m	234	–	–	454	4.65 (4.90)
CoAcAMDH $\cdot$ 2H_2O	3254 sh	2995 sh	1643 s	1540 s	1373 m	235	253	271	496	3.71 (3.87)
NiAcAMDH $\cdot$ H_2O	3246 sh	3030 w	1640 s	1531 s	1373 m	223	232	–	619	2.65 (2.83)
CuAcAMDH $\cdot$ H_2O	3224 sh	3020 sh	1645 s	1533 s	1373 m	235	244	–	650	1.62 (1.73)
ZnAcAMDH $\cdot$ 2.5H_2O	3244 sh	3030 w	1648 s	1539 s	1371 m	242	–	–	–	–

[a] IR frequencies in cm^{-1}. s: strong; m: medium; sh: shoulder; w: weak.

[b] Spin-only values in parentheses.

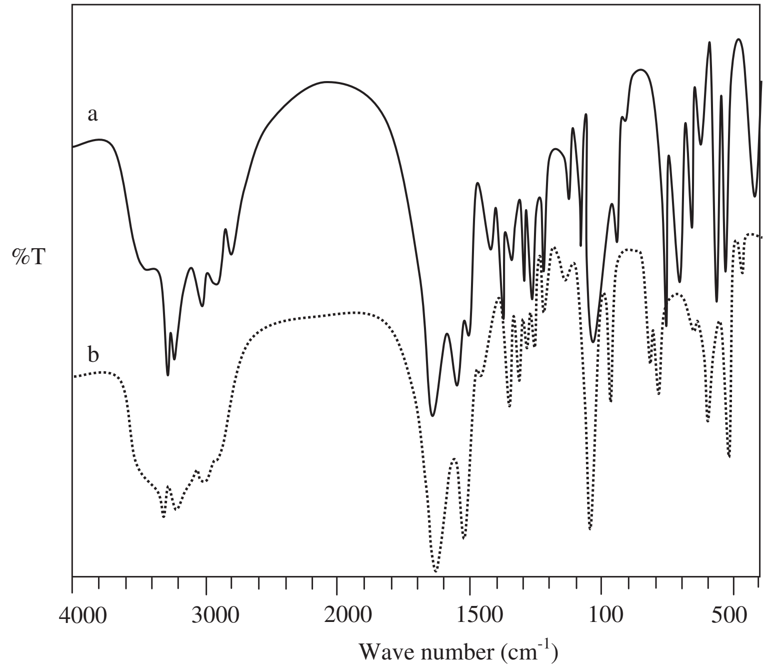

FIGURE 2 FTIR spectra of K_2AcAMDH · 1.5H_2O (a) and MnAcAMDH · 5.5H_2O (b).

TABLE III Thermoanalytical data for K_2AcAMDH · 1.5H_2O and the metal complexes

Compound	*Temp. range (°C)*	*DTA_{max} (°C)*	*Mass loss (%)*		*Total mass loss (%)*		*Solid residue*
			Found	*Calcd.*	*Found*	*Calcd.*	
K_2AcAMDH · 1.5H_2O	26–135	50(+)	8.8	9.2			K_2AcAMDH
	140–180	174(−)	37.8	–			–
	180–980	390(−), 500(−), 867(−)	53.4	–	100.0	100.0	–
MnAcAMDH · 5.5H_2O	40–96	70(+)	15.5	15.7			MnAcAMDH · 2.5H_2O
	99–167	132(+)	13.0	13.1			MnAcAMDH
	170–940	202(−), 339(−), 404(−)	50.2	50.4	78.7	79.2	MnO
FeAcAMDH · 3H_2O	30–106	58(+)	18.3	18.1			FeAcAMDH
	125–590	173(−), 366(−)	54.8	55.2	73.1	73.3	Fe_2O_3
CoAcAMDH · 2H_2O	36–134	73(+)	12.5	12.7			CoAcAMDH
	140–510	280(−), 427(−)	58.0	58.1	70.5	70.9	Co_2O_3
NiAcAMDH · H_2O	42–114	62(+)	7.0	6.8			NiAcAMDH
	120–910	181(−), 254(−), 504(−)	64.6	65.1	71.6	71.9	NiO
CuAcAMDH · H_2O	40–113	69(+)	6.8	6.7			CuAcAMDH
	184–430	243(−), 391(−)	63.1	64.0	69.9	70.7	CuO
ZnAcAMDH · 2.5H_2O	82–162	138(+)	14.8	15.0			ZnAcAMDH
	172–557	209(−), 303(−), 447(−)	57.7	57.8	72.5	72.8	ZnO

(+), endothermic; (−), exothermic.

in Table III. $K_2AcAMDH \cdot 1.5H_2O$ dehydrates at 50°C and decomposes exothermically in the temperature range 140–980°C. A large part of the compound with a mass of 37.8% is eliminated between 140 and 180°C with a sharp exothermic DTA peak at 174°C, and the decomposition of the solid residue formed at around 180°C occurs with a slow mass loss at higher temperatures leaving an empty crucible. The DTA, TG and DTG curves clearly indicate that the metal complexes exhibit similar thermal decomposition behaviour. The first stage of decomposition corresponds to the endothermic dehydration of the complexes. The mass loss values for the dehydration stages agree well with the calculated values (Table III). The anhydrous complexes are stable within a small temperature range, and then undergo a strong exothermic degradation in two or three steps to give the corresponding metal oxides as the final decomposition products at around 500 to 1000°C. The total mass losses are consistent with the calculated values. Formation of metal oxides in the nitrogen atmosphere suggests the presence of reasonably strong covalent metal–oxygen bonds.

Electrochemical Behavior

The ligand is electrochemically inactive, but the aqueous solution of the ligand is stable up to only *ca.* 12 hours. Therefore, each measurement was performed using freshly prepared ligand solutions. Copper(II) and zinc(II) form labile complexes with AcAMDH whereas iron(II) and nickel(II) form inert complexes (see Fig. 3). Experimentally, the inert character of the iron(II) and nickel(II) complexes was detected when the addition

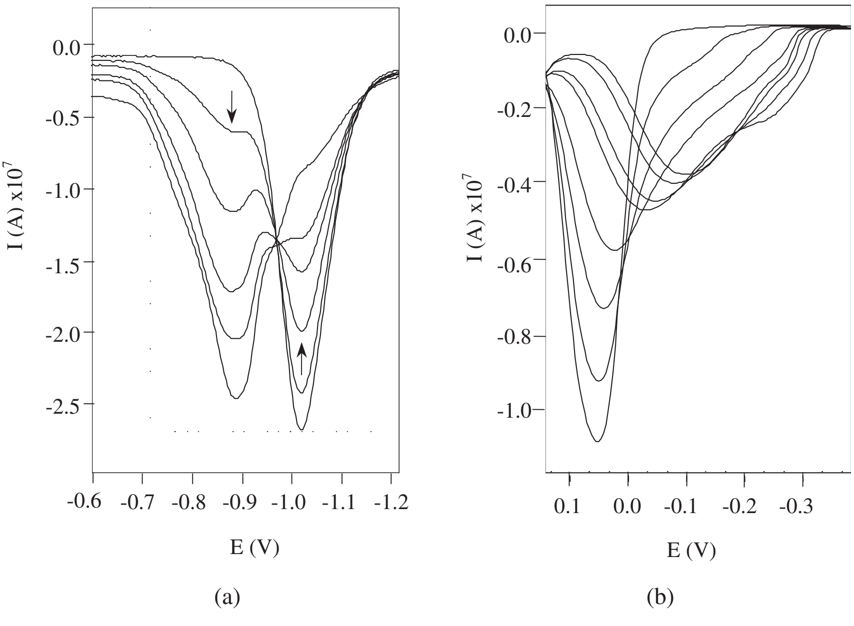

(a) (b)

FIGURE 3 SWV voltammograms of the nickel(II) (a) and copper(II) (b) complexes with increasing metal to ligand ratios at neutral pH.

of the ligand to the metal ions produced a progressive decrease in the peak current and no shift in the peak potentials. Additionally, new peaks occurred due to formation of these inert complexes. The metal : ligand ratios of the iron(II) and nickel(II) complexes were found from the change in complex peak currents with the addition of the ligand to metal solutions, as illustrated in Fig. 4. Although this method only works for ideal systems, in this case it was found to be suitable for estimating the metal : ligand ratios. The complex stability constants and the metal : ligand ratios of copper(II) and zinc(II) complexes were calculated by the Deford–Hume method [16,17]. Observations show that the metal to ligand mol ratio is 1 : 1 in the iron(II) and nickel(II) complexes but 1 : 2 in the copper(II) and zinc(II) complexes. The complexation mechanism in solution was clearly shown to differ from that in the solid state and it is assumed that the copper(II) and zinc(II) ions are coordinated by two AcAMDH ligands forming the stable $[ML_2]^{2-}$ complex species in solution, although they are isolated as the solid complexes with a metal to ligand mol ratio of 1 : 1. In contrast to other metals, the addition of the ligand to the manganese(II) and cobalt(II) solutions did not cause any shift in peak potentials or a new complex peak. Therefore, neither stoichiometry nor a stability constant could be estimated for these metal ions under the experimental conditions. This may be due to low concentrations of the reactants or the strength of interaction between the aqua ligand and these metals in solution.

Typical CV voltammograms of the successive complexes are shown in Fig. 5. The copper(II) and zinc(II) complexes produce both cathodic and anodic peaks with a reversible electrode process, whereas the iron(II) and nickel(II) complexes yield only a cathodic reduction peak due to irreversibility. From the log plots of the sampled DC polarograms of the metal complexes [18], the αn values of the electrode reactions were calculated and found to be in agreement with CV results (Table IV). As the

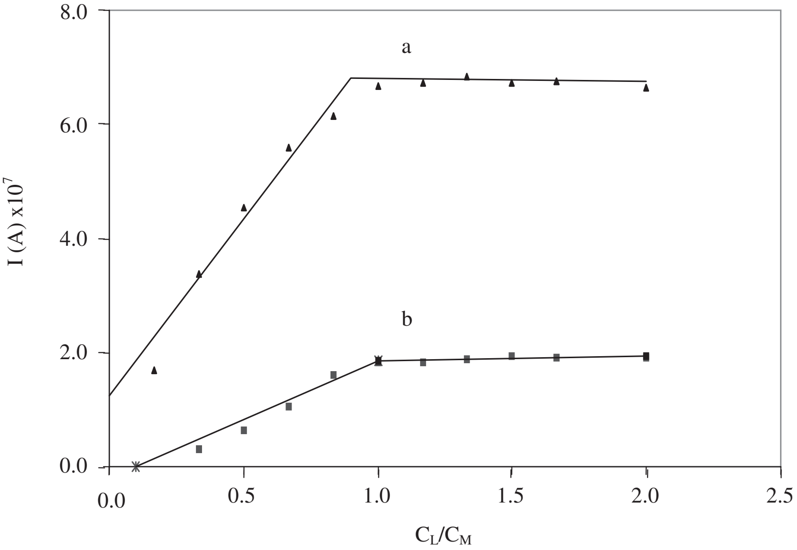

FIGURE 4 Variation in peak currents with different ligand to metal ratios in the iron(II) (a) and nickel(II) (b) complexes.

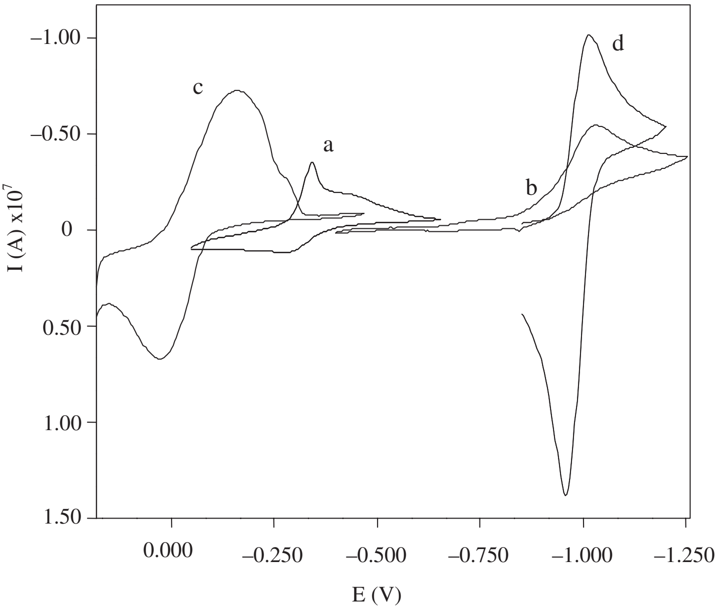

FIGURE 5 CV voltammograms of the metal(II)–AcAMDH complexes with (a) iron(II), (b) nickel(II), (c) copper(II) and (d) zinc(II) at twofold excess of the ligand relative to the metal ions and neutral pH (scan rate $100\,mV\,s^{-1}$).

TABLE IV Voltammetric data and stability constants for the metal complexes of AcAMDH

Complex	*E_p–complex/mV*	*αn*	*M : L mol ratio*	*log β*
Fe–AcAMDH	−0.320	0.97	1 : 1	8.03
Ni–AcAMDH	−0.851	0.60	1 : 1	7.82
Cu–AcAMDH	−0.125	1.33	1 : 2	12.47
Zn–AcAMDH	−1.010	1.77	1 : 2	9.00

electron number (*n*) of the metal ions used in the electrochemical reactions is two, *αn* values indicate the reversibility of electrode reactions. The reversibility of the copper(II) and zinc(II) complexes is greater than that of the iron(II) and nickel(II) complexes. This is also shown in the CV voltammograms of the complexes: the anodic peak to the cathodic peak ratio is very close to 1 in the copper(II) and zinc(II) complexes, but much smaller in the iron(II) and nickel(II) complexes.

Earlier studies suggested that dihydroxamic acid ligands, in general, exhibit a greater tendency to form dimeric species in solution [15,19,20]. However, the coordination modes of dihydroxamate ions were not discussed in the solid state and in one case an iron(III)–trihydroxamate complex was reported to be polynuclear [21]. In our case the insolubility of the metal complexes strongly suggests the formation of solid polymeric complexes as proposed in Fig. 6. The AcAMDH acts as a bis-chelate tetradentate ligand through two hydroxamate groups to form a polynuclear chain. Two water molecules coordinate to manganese(II), iron(II) and cobalt(II) ions, resulting in an octahedral coordination. Although the formation of pyramidal geometry may also be

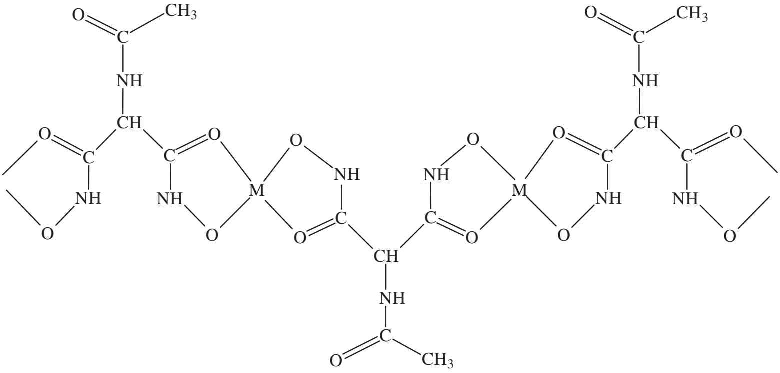

FIGURE 6 The suggested polymeric structure of the metal complexes of AcAMDH.

expected with coordination of a water molecule, the other complexes were thought to have tetrahedral coordination.

Acknowledgment

We are grateful to Ondokuz Mayis University for the financial support given to this research project.

References

[1] K.N. Raymond, *Pure Appl. Chem.* **66**, 773 (1994).
[2] A.M. Albrecht-Gary and A.L. Crumblis, In: A. Sigel and H. Sigel (Eds), Metal Ions in Biological Systems in Iron Transport and Storage in Microorganisms, Plants and Animals (M. Dekker, New York, 1998), Vol. 35, p. 239.
[3] D.A. Brown, H. Bogge, R. Coogan, D. Doocey, T.J. Kemp, A. Muller and B. Neumann, *Inorg. Chem.* **36**, 1674 (1996).
[4] E. Kehl, Chemistry and Biology of Hydroxamic Acids (S. Karger, New York, 1982).
[5] B. Chatterjee, *Coord. Chem. Rev.* **26**, 281 (1978).
[6] B. Kurzak, H. Kozlowski and E. Farkas, *Coord. Chem. Rev.* **114**, 169 (1992).
[7] C.P. Brink and A.L. Crumblis, *Inorg. Chem.* **24**, 4708 (1984).
[8] V.T. Yilmaz and F. Yilmaz, *Transition Met. Chem.* **23**, 726 (1999).
[9] V.T. Yilmaz and F. Yilmaz, *Thermochim. Acta* **348**, 139 (2000).
[10] F. Yilmaz and V.T. Yilmaz, *Synth. React. Inorg. Met.-Org. Chem.* **31**, 1421 (2001).
[11] F. Yilmaz, V.T. Yilmaz, S. Topcu and N. Menek, *J. Coord. Chem.* **56**, 903 (2003).
[12] M.A. Santos, R. Grazina, M. Pinto and E. Farkas, *Inorg. Chim. Acta* **321**, 42 (2001).
[13] M.K. Nguyen-van-Duong, V. Guillot, L. Nicolas, A. Gaudemer, L. Lowry, I. Spasojevic and A.L. Crumblis, *Inorg. Chem.* **40**, 5948 (2001).
[14] E.Q. Adams, *J. Am. Chem. Soc.* **38**, 1503 (1916).
[15] E. Farkas, E.A. Enyedy and H. Csoka, *Polyhedron* **18**, 2391 (1999).
[16] D. Deford and D.H. Hume, *J. Am. Chem. Soc.* **73**, 532 (1951).
[17] D.R. Crown, Polarography of Metal Complexes (Academic Press, London, 1969), pp. 56–64.
[18] A.J. Bard and L.R. Faulkner, Electrochemical Methods: Fundamentals and Applications (Wiley, New York, 1980), pp. 163–172.
[19] M.T. Caudle, L.P. Cogswell and A.L. Crumblis, *Inorg. Chem.* **33**, 4759 (1994).
[20] M.T. Caudle, R.D. Stevens and A.L. Crumblis, *Inorg. Chem.* **33**, 6111 (1994).
[21] I. Dayan, J. Libman, Y. Agi and A. Shanzer, *Inorg. Chem.* **32**, 1467 (1993).